Supporting Information for: *Ab initio* Monte Carlo prediction of chemical order and disorder in multicomponent MXenes

Noah Oyeniran[1], Chongze Hu[1,*]

1. Department of Aerospace Engineering and Mechanics, University of Alabama, Tuscaloosa, AL 35406, USA
*Corresponding author email: hucz@ua.edu

Contents

Supplementary Note 1: DFT/MC framework comparison

Supplementary Figure S1 shows the energy evolution of DFT/MC-simulated structures with varying coordination environments during convergence to the minimum-energy configuration (MEC). The energy profiles of three MXene systems from the present and previous DFT/MC simulations framework are plotted for comparison. For all DFT/MC simulations, $3 \times 3 \times 1$ supercells were used for $(Ti_{0.5}Mo_{0.5})_4C_3$ with octahedral coordination, $(Ti_{0.5}Mo_{0.5})_4C_3$ with OOPOO coordination, and $(Ti_{0.75}Mo_{0.25})_4C_3$ with prismatic coordination.

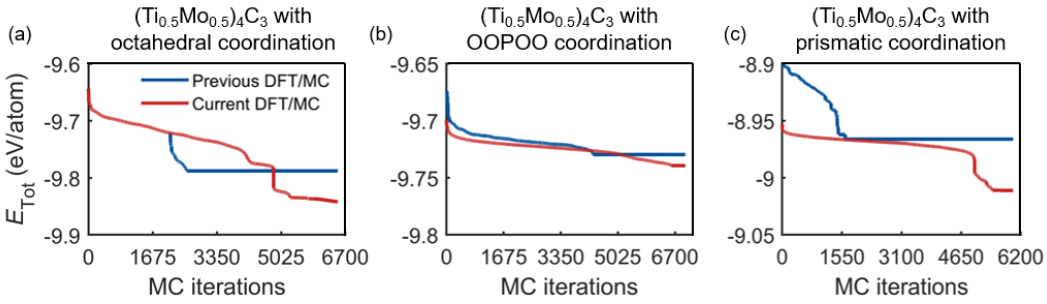

Supplementary Figure S1: Energy profiles during DFT/MC iterations using previous and current DFT/MC framework for: (a) $(Ti_{0.5}Mo_{0.5})_4C_3$ with octahedral coordination, (b) $(Ti_{0.5}Mo_{0.5})_4C_3$ with OOPOO coordination, and (c) $(Ti_{0.75}Mo_{0.25})_4C_3$ with prismatic coordination. Each system displays the number of MC iterations at which MEC is observed, which is indicated by a long, straight convergence line.

Supplementary Note 2: Electronic structures of three representative (TiMo)-based carbide MXenes

Supplementary Figure S2 shows electronic density of states (DOS) of three representative (TiMo)-based MXenes, including (a) the bare $(Ti_{0.5}Mo_{0.5})_4C_3$ MXene, and (b-c) terminated MXenes $(Ti_{0.5}Mo_{0.5})_4C_3F_2$ with F termination and $(Ti_{0.5}Mo_{0.5})_4C_3O_2$ with O termination. The spin polarization is included in all electronic structure calculations, and the nearly same spin-up and spin-down DOS indicate that the magnetization is very small for (TiMo)-based MXenes. Thus, spin polarization is not considered in the DFT/MC screening process.

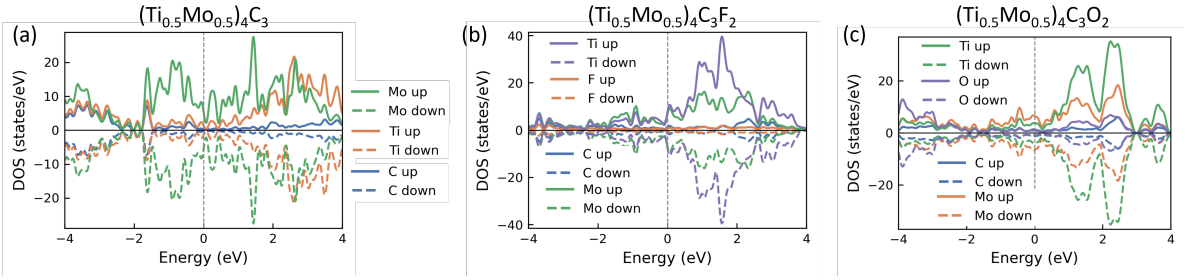

Supplementary Figure S2: Electronic partial density of states (PDOS) of (a) bare $(Ti_{0.5}Mo_{0.5})_4C_3$ MXene, and (b-c) terminated MXenes $(Ti_{0.5}Mo_{0.5})_4C_3F_2$ with F termination and $(Ti_{0.5}Mo_{0.5})_4C_3O_2$ with O termination.

Supplementary Note 3: Energy profiles of DFT/MC simulations for MXene structures with varying termination elements and coordination environments

Supplementary Figure S3 shows the energy profile of DFT/MC-simulated structures with varying termination elements and coordination environments until convergence to the minimum energy configuration (MEC). For all DFT/MC simulations, $3 \times 3 \times 1$ supercells were used for $(Ti_{0.5}Mo_{0.5})_4C_3F_2$ with octahedral coordination of M' sites, $(Ti_{0.5}Mo_{0.5})_4C_3O_2$ with octahedral coordination of M' sites, $(Ti_{0.5}Mo_{0.5})_4C_3F_2$ with prismatic coordination of M' sites, and $(Ti_{0.5}Mo_{0.5})_4C_3O_2$ with prismatic coordination of M' sites.

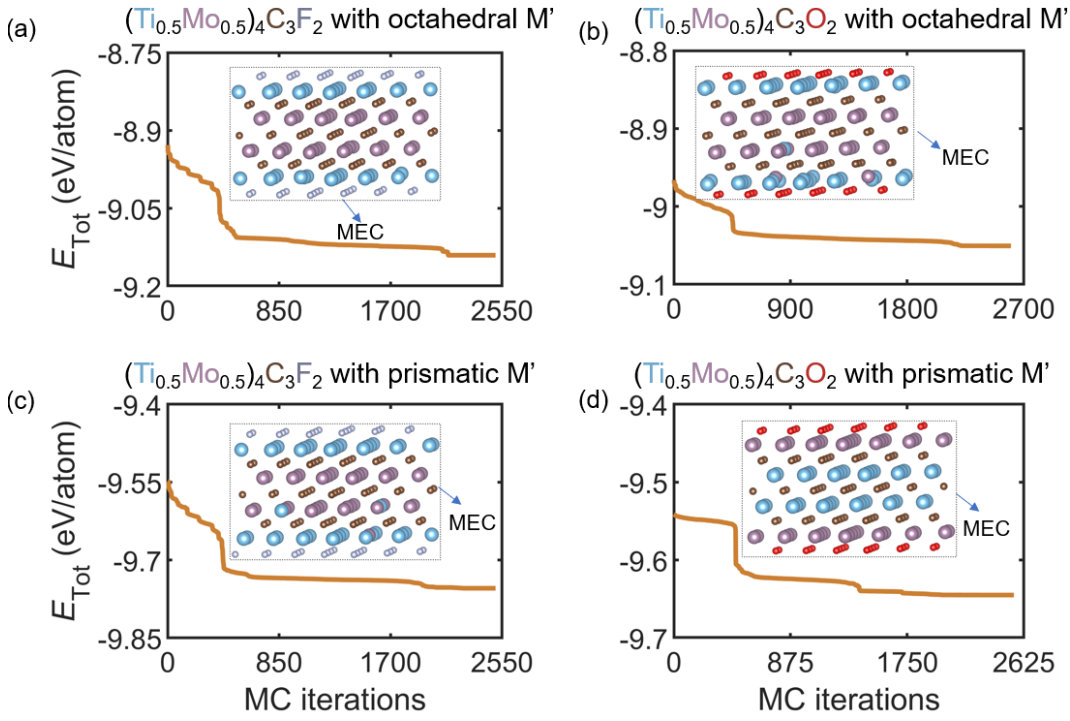

Supplementary Figure S3: Energy profiles during DFT/MC iterations and the resulting MC-searched minimum-energy configurations (MECs) for: (a) $(Ti_{0.5}Mo_{0.5})_4C_3F_2$ with octahedral coordination of M' sites, (b) $(Ti_{0.5}Mo_{0.5})_4C_3O_2$ with octahedral coordination of M' sites, (c) $(Ti_{0.5}Mo_{0.5})_4C_3F_2$ with prismatic coordination of M' sites, and (d) $(Ti_{0.5}Mo_{0.5})_4C_3O_2$ with prismatic coordination of M' sites. Each system displays the number of MC iterations at which MEC is observed, which is indicated by a long, straight convergence line.

Supplementary Note 4: Energy profiles of DFT/MC simulations of MXene structures terminated with different oxygen/fluorine (O/F) ratios.

Supplementary Figure S4 shows DFT/MC-simulated $(Ti_{0.5}Mo_{0.5})_4C_3F_2$ with progressively increasing oxygen-termination concentration on an initially F-terminated surface. All simulations were performed using $3\times3\times1$ supercells. The resulting energy profiles demonstrate convergence toward a minimum-energy configuration for each termination level.

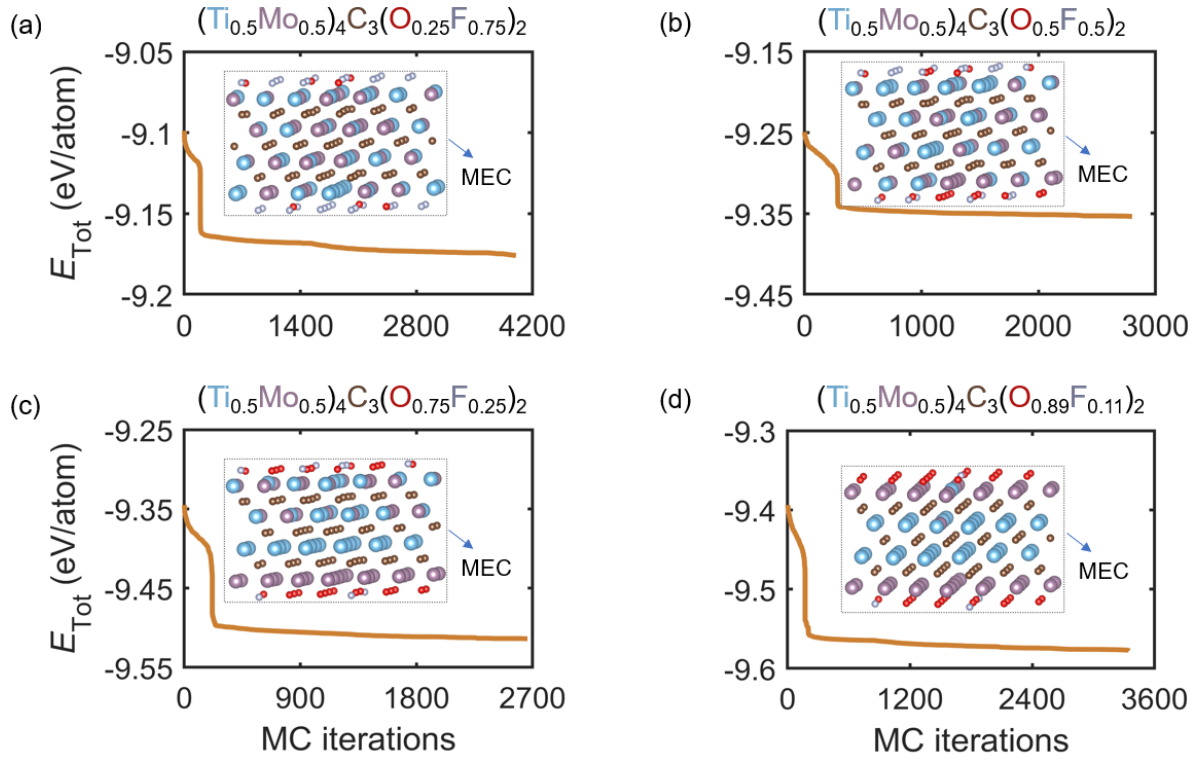

Supplementary Figure S4: The energy profile during MC iterations and the MC-searched stable configuration of M' prismatic coordination of (a) $(Ti_{0.5}Mo_{0.5})_4C_3(O_{0.25}F_{0.75})_2$, (b) $(Ti_{0.5}Mo_{0.5})_4C_3(O_{0.50}F_{0.50})_2$, (c) $(Ti_{0.5}Mo_{0.5})_4C_3(O_{0.75}F_{0.25})_2$, and (d) $(Ti_{0.5}Mo_{0.5})_4C_3(O_{0.89}F_{0.11})_2$. The trends show convergence to MECs.

Supplementary Note 5: Energy profiles of DFT/MC simulations of $(Ti_{0.5}Mo_{0.5})_4C_3$ MXenes with different coordination environments

Supplementary Figure S5 shows DFT/MC-simulated $(Ti_{0.5}Mo_{0.5})_4C_3$ with different coordination environments. The $3\times3\times1$ supercells were used in these MC simulations. The energy trend path shows the journey of the MC simulation to finding MECs. The MEC for each corresponding coordination arrangement is shown as an inset in each plot.

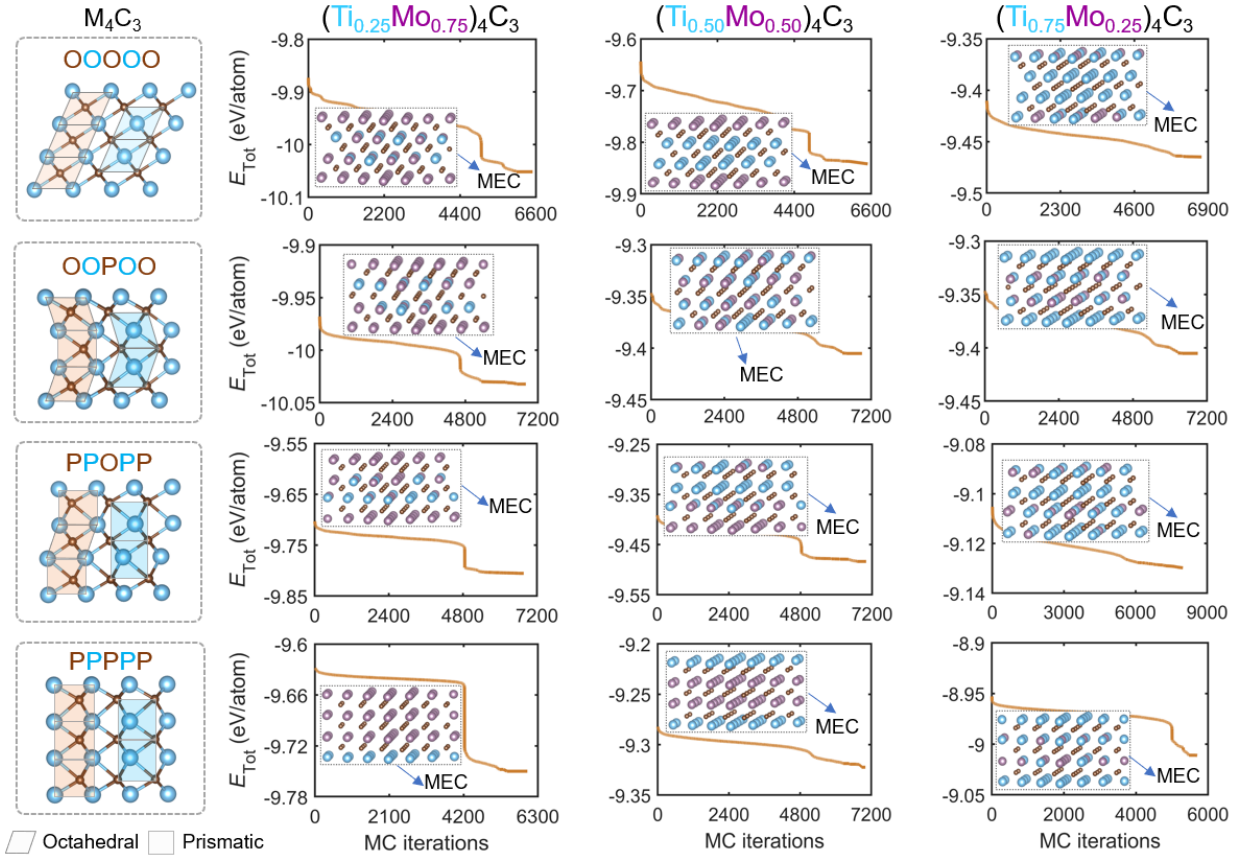

Supplementary Figure S5: The energy profile during MC iterations and the MC-searched stable configuration of $(Ti_{0.5}Mo_{0.5})_4C_3$. Each row represents an increase in Ti content, while each column illustrates the gradual transition from an initially octahedrally dominated structure to one with increasing prismatic coordination, ultimately reaching a fully prismatic configuration. This structural arrangement is illustrated in the first column, which provides the reference structure for each row.

Supplementary Table S1: **DFT-calculated lattice parameters and average bond lengths (in Å) for $(Ti_{0.5}Mo_{0.5})_4C_3T_2$ MXenes with different terminations and coordination environments. The first row is the experimentally reported data from Ref. [1].**

MXene Type	**Lattice (Å)**		**Mo–C (Å)**		**Ti–C (Å)**		**Mo–T_x / Ti–T_x (Å)**	
	a	**b**	**Avg**	**Std**	**Avg**	**Std**	**Avg**	**Std**
$(Ti_{0.5}Mo_{0.5})_4C_3O_2$ (exp)	2.96	-	2.13	-	2.11	-	1.92	-
$(Ti_{0.5}Mo_{0.5})_4C_3F_2$ (Oct)	3.07	3.07	2.19	0.04	2.07	0.00	2.18	0.00
$(Ti_{0.5}Mo_{0.5})_4C_3F_2$ (Pris)	3.02	3.02	2.17	0.03	2.10	0.02	2.20 / 2.28	0.00 / 0.01
$(Ti_{0.5}Mo_{0.5})_4C_3O_2$ (Oct)	3.04	3.04	2.25	0.32	2.19	0.07	2.31	0.65
$(Ti_{0.5}Mo_{0.5})_4C_3O_2$ (Pris)	2.96	2.96	2.14	0.00	2.14	0.01	2.09	0.00
$(Ti_{0.5}Mo_{0.5})_4C_3(O_{0.25}F_{0.75})_2$	3.00	3.00	2.15	0.04	2.14	0.03	2.18 / 2.25	0.01 / 0.01
$(Ti_{0.5}Mo_{0.5})_4C_3(O_{0.5}F_{0.5})_2$	2.99	2.99	2.22	0.31	2.14	0.02	2.18 / 2.25	0.01 / 0.02
$(Ti_{0.5}Mo_{0.5})_4C_3(O_{0.75}F_{0.25})_2$	2.98	2.98	2.18	0.25	2.15	0.03	2.16 / 2.25	0.01 / 0.01
$(Ti_{0.5}Mo_{0.5})_4C_3(O_{0.89}F_{0.11})_2$	2.97	2.97	2.14	0.02	2.14	0.02	2.20 / 2.23	0.00 / 0.01

Acknowledgements

N.O., and C.H. acknowledge the support of DOE Award DE-SC0025431. This research used resources of the National Energy Research Scientific Computing Center, a DOE Office of Science User Facility supported by the Office of Science of the U.S. Department of Energy under Contract No. DE-AC02-05CH11231 using NERSC award BES-ERCAP0031213. This work was also supported by a user project at the Center for Nanophase Materials Sciences (CNMS), a US DOE Office of Science User Facility, operated at Oak Ridge National Laboratory. Computations used resources of the National Energy Research Scientific Computing Center (NERSC), a US DOE Office of Science User Facility using NERSC award BES-ERCAP0027465 and ERCAP0031261 and BES-ERCAP35988.

References

Supplementary References

[1] Babak Anasori, Chenyang Shi, Eun Ju Moon, Yu Xie, Cooper A Voigt, Paul RC Kent, Steven J May, Simon JL Billinge, Michel W Barsoum, and Yury Gogotsi. Control of electronic properties of 2d carbides (mxenes) by manipulating their transition metal layers. *Nanoscale Horizons*, 1(3):227–234, 2016.